

Multi-Scale Attention and Gated Shifting for Fine-Grained Event Spotting in Videos

Hao Xu
Deakin University
Melbourne, Australia

august.xu@research.deakin.edu.au

Sam Wells
Paralympics Australia
Melbourne, Australia

sam.wells@paralympic.org.au

Richard Dazeley
Deakin University
Melbourne, Australia

richard.dazeley@deakin.edu.au

Arbind Agrahari Baniya
Deakin University
Melbourne, Australia

a.agraharibaniya@deakin.edu.au

Mohamed Reda Bouadjenek
Deakin University
Melbourne, Australia

reda.bouadjenek@deakin.edu.au

Sunil Aryal
Deakin University
Melbourne, Australia

sunil.aryal@deakin.edu.au

Abstract

*Precise Event Spotting (PES) in sports videos requires frame-level recognition of fine-grained actions from single-camera footage. Existing PES models typically incorporate lightweight temporal modules such as Gate Shift Module (GSM) or Gate Shift Fuse (GSF) to enrich 2D CNN feature extractors with temporal context. However, these modules are limited in both temporal receptive field and spatial adaptability. We propose a **Multi-Scale Attention Gate Shift Module (MSAGSM)** that enhances GSM with multi-scale temporal dilations and multi-head spatial attention, enabling efficient modeling of both short- and long-term dependencies while focusing on salient regions. MSAGSM is a lightweight plug-and-play module that can be easily integrated with various 2D backbones. To further advance the field, we introduce the **Table Tennis Australia (TTA) dataset**—the first PES benchmark for table tennis—containing over 4,800 precisely annotated events. Extensive experiments across five PES benchmarks demonstrate that MSAGSM consistently improves performance with minimal overhead, setting new state-of-the-art results.*

1. Introduction

Detecting the precise moment when events occur in a video is a core challenge in video understanding, particularly in

the single-camera setting commonly used in most sports recordings. Precise Event Spotting (PES) aims to localize and classify events at frame-level accuracy, typically within a 1–2 frame tolerance [11]. This fine-grained precision is critical in sports scenarios, where even a few frames of deviation can correspond to a different event entirely (see Figure 1). Accurate PES provides a strong foundation for downstream tasks such as ball tracking, player positioning, and automatic highlight generation. Moreover, precise spotting plays a vital role in post-game analysis by surfacing key moments and reducing the need to manually browse full-length videos. For instance, according to Table Tennis Australia’s sports analytics team, annotating events in a single match video can take 4–5 hours. Automating this process not only streamlines analysis but also enables timely feedback for athletes and coaches.

Recent advancements in video understanding have explored various approaches to this task, including transformer-based models [1, 41], multi-modal methods [30, 34], and self-supervised frameworks [4]. Among these, E2E-Spot [11] has emerged as a strong baseline, inspiring several subsequent models such as the current state-of-the-art T-DEED [35] and UGLF [29]. A key component in E2E-Spot is the Gate Shift Module (GSM) [25], which enables 2D CNNs to learn temporal dynamics by shifting features across adjacent frames. While effective, GSM is limited in its temporal range and does not explicitly model longer-term dependencies.

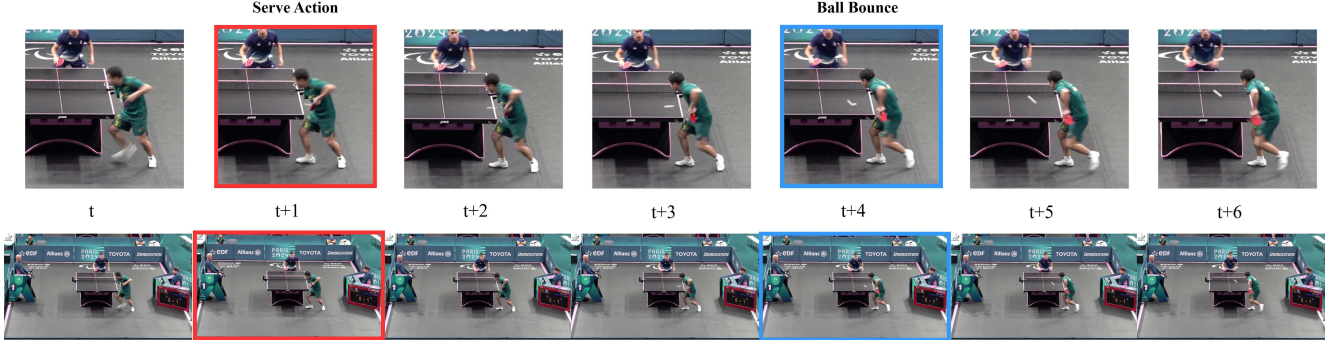


Figure 1. Example of Precise Event Spotting: in table tennis, the moment a player contacts the ball during a serve (red) or when a ball bounces on the table (blue).

Despite these advancements, PES remains a highly challenging task due to its unique characteristics. Events are often difficult to distinguish from adjacent frames—sometimes even for human annotators—without access to extended temporal context [35]. Moreover, different events may require varying amounts of temporal information to be correctly identified, further complicating model design. In addition to temporal reasoning, effective PES also demands accurate spatial attention: in sports videos, a large portion of each frame typically consists of background, making it essential for models to focus on small but informative regions—such as the ball or a player’s hand position—to make correct predictions. Another practical limitation lies in the availability of suitable datasets. Most publicly available sports video datasets are derived from broadcast footage of elite sports [8, 10, 11, 38], which are often professionally edited and filmed from ideal angles. However, in many real-world sports settings—such as local or developmental leagues—matches are recorded using handheld devices with varied perspectives, inconsistent quality, and frequent occlusions.

To address these challenges, we propose the Multi-Scaled Attention Gate Shift Module (MSAGSM), a lightweight module that enhances the temporal modeling capacity of 2D CNNs. MSAGSM builds upon the GSM framework by incorporating multi-scale temporal shifts and attention mechanisms. This design allows the model to capture longer-range dependencies while simultaneously attending to important spatial regions such as the ball or player positions. Importantly, MSAGSM is computationally efficient and can be easily integrated into existing 2D backbones without the resource overhead associated with 3D models.

In addition, we introduce a new dataset for PES: the Table Tennis Australia (TTA) dataset, recorded and curated in collaboration with Paralympics Australia’s sports analysts. The dataset includes 39 games and a total of 4,878 annotated events across eight event types: serve, bounce,

forehand, and backhand—each distinguished between the near and far sides of the table. To our knowledge, TTA is the first PES dataset specifically designed for table tennis. Compared to existing PES datasets, TTA is both sizable and challenging. Its scale is comparable to FineGym [22] and surpasses that of FineDiving [38] and FigureSkating [10]. Moreover, unlike tennis [11], table tennis involves more densely packed, fine-grained events within shorter time spans, presenting a more demanding benchmark for precise spotting.

Our main contributions are summarized as follows: (1) We propose **MSAGSM**, a lightweight module that combines multi-scale temporal shifts with spatial attention, and can be efficiently plugged into existing 2D CNN backbones. (2) We introduce the **Table Tennis Australia (TTA)** dataset, the first PES dataset for table tennis, containing 39 games and 4,878 annotated events across 8 classes. (3) MSAGSM, when integrated with standard 2D backbones, achieves state-of-the-art performance across multiple PES benchmarks, including TTA.

2. Related Work

Spatial-Temporal Modelling Significant progress has been made in video understanding tasks—such as video classification and action recognition—driven by the development of deep convolutional neural networks (CNNs) and Transformer-based architectures [2, 5, 6, 17, 27]. One major challenge in these models is their high memory and computational requirements, which make them less suitable for deployment on resource-constrained devices compared to lightweight 2D CNNs.

To address this, recent research has focused on developing efficient and effective temporal modeling techniques built on top of 2D CNNs, minimizing computational complexity while retaining performance. Several approaches attempt to decompose 3D convolutions into separate spatial (2D) and temporal (1D) components [12, 20, 28, 36]. Others propose hybrid models that combine 3D CNNs with 2D

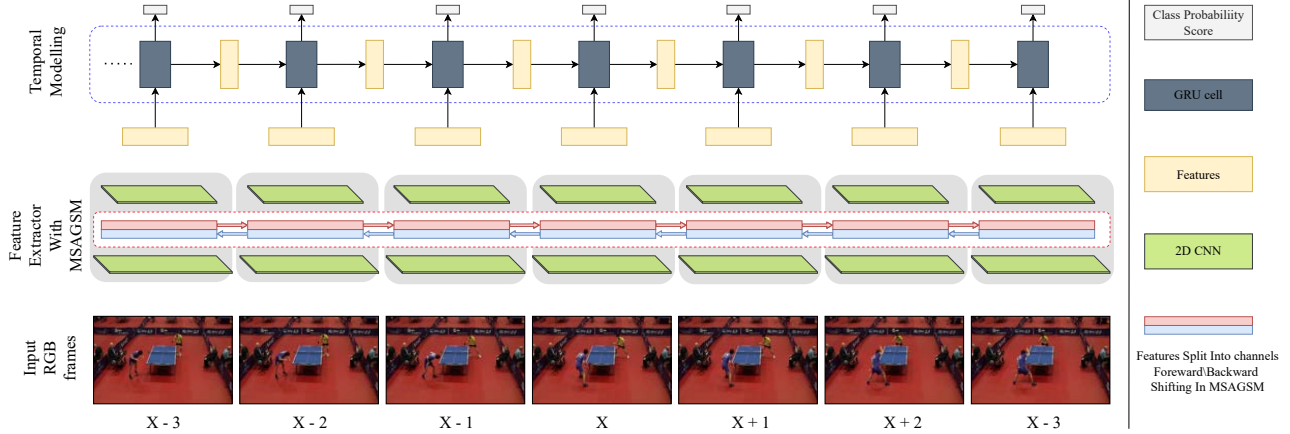


Figure 2. Overview of our proposed architecture for Precise Event Spotting (PES). The input video is processed through a 2D CNN backbone for spatial feature extraction, followed by the Multi-Scaled Attention Gate Shift Module (MSAGSM) for spatio-temporal modeling. MSAGSM combines channel-wise attention and multi-scale temporal shifting to capture varying temporal dependencies. The resulting features are passed through a GRU-based temporal model to predict event class probabilities at the frame level.

CNNs to reduce overall cost [19].

A key advancement in this direction is the Temporal Shift Module (TSM) [15], which enables 2D CNNs to capture temporal information by shifting a portion of the feature channels along the temporal dimension. This parameter-free operation significantly improves efficiency over 3D or 2D+1D methods and demonstrated state-of-the-art performance in action recognition at the time. However, TSM’s shift mechanism is manually hardcoded and does not adapt to the input content.

To address this limitation, the Gate Shift Module (GSM) [25] was introduced. Built upon TSM, GSM employs an additional spatio-temporal 3D convolutional kernel as a gating mechanism to selectively decide which features to shift forward or backward based on contextual information. Its variant, Gate Shift Fuse (GSF) [26], adds a point-wise convolution block before and after the gating operation to enable interaction between spatial and spatio-temporal feature groups, further enhancing modeling capability.

Precise Event Spotting In video understanding tasks such as video classification and action recognition, a common approach is to *sparsely* sample frames from the entire video [7, 13, 31]. In contrast, Precise Event Spotting (PES) requires *dense* frame sampling—particularly for sports videos—due to the fast motion and high frequency of events occurring within short time spans.

Compared to Temporal Action Detection (TAD), which focuses on predicting temporal intervals of actions [16, 24], PES aims to identify actions using a single key frame. This is especially relevant in sports scenarios, where the start and end boundaries of actions (e.g., a forehand shot) can be visually ambiguous and difficult to define precisely [37].

To address this ambiguity, the SoccerNet dataset intro-

duced the task of Action Spotting (AS) [8], which focuses on identifying key frames of important events within a relaxed temporal window (e.g., ± 50 frames). Subsequently, PES was proposed to enforce a stricter temporal tolerance, requiring models to be accurate within just a few frames.

E2E-Spot [11] serves as a strong PES baseline, combining RegNetY with the Gate Shift Module (GSM) for temporal modeling. Building on this, T-DEED [35] addressed the challenge of distinguishing between adjacent frames with highly similar visual appearance. It incorporated the Scalable Granularity Perception (SGP) module [23] to enhance discriminability among temporally close features.

UGLF [29] takes a different direction by incorporating the vision-language model GLIP [14]. GLIP processes both an image and a textual prompt to extract meaningful object-level features such as ‘ball’, ‘referee’, or ‘card’, marking the first use of vision-language models in the PES domain.

Beyond visual features, audio signals can also serve as important cues in sports—for instance, crowd noise after a goal or racket contact sound in tennis. ASTRA [34], a transformer-based encoder-decoder model designed for soccer, integrates both visual and audio embeddings, using learnable queries in the decoder to jointly attend to multi-modal cues.

PES Datasets Existing datasets are often acquired from broadcast videos from high-level matches such as [8, 10, 11, 22, 38]. These datasets are fine-grained, where all event and class labels relate to a single activity.

Despite progress, existing models often fail to capture both short- and long-range temporal dependencies while attending to relevant spatial regions. They also rely on broadcast-quality footage, limiting applicability in grassroots or para-sports where handheld cameras are used.

To address this, we propose the **Multi-Scaled Attention Gate Shift Module (MSAGSM)**, a lightweight temporal modeling block, and introduce **Table Tennis Australia (TTA)**—the first PES benchmark for table tennis, captured in real-world conditions using single-camera recordings by sports analysts.

3. Multi-Scale Attention GSM

3.1. Overview

Our approach enables 2D CNNs to capture varying spatio-temporal dependencies through an efficient combination of multi-scale gated shifting and attention mechanisms. The proposed method consists of two main components: (1) A multi-head attention module, which splits the input features into multiple groups and applies attention independently to each group, allowing the model to focus on spatially informative regions; (2) A multi-scale GSM, which introduces temporal dilations to shift features across varying temporal distances. This design allows the model to directly access a broader temporal context compared to the original GSM. An overview of the module architecture is illustrated in Figure 2.

3.2. Attention GSM

Our intuition is rooted in the observation that, in sports videos, most critical events are concentrated around key entities such as players, referees, and the ball. In contrast, a large portion of each frame consists of background content that contributes little to event detection. Motivated by the effectiveness of attention mechanisms in prior work [3, 5, 32, 33], we extend the original GSM into a **multi-head attention GSM**. This design allows the model to focus on spatially informative regions while suppressing irrelevant background, thereby improving the accuracy of event spotting. Figure 3 shows the details of spatial attention,

We generate spatial attention maps using 2D convolutional layers to highlight the most informative regions within a feature map. Given an intermediate feature tensor, we first split it into multiple chunks along the channel dimension, where the number of chunks corresponds to a predefined number of attention heads—a tunable hyperparameter.

The motivation behind using multiple spatial attention heads is to account for the varying number of salient regions required across different sports. For example, in tennis, the model must simultaneously attend to multiple entities such as two players and a fast-moving ball, whereas in diving, the focus is typically on a single athlete. Conventional spatial attention mechanisms produce a single attention map, which limits the model’s capacity to flexibly adapt to such variation. In contrast, our multi-head design enables the model to learn multiple independent attention maps, allow-

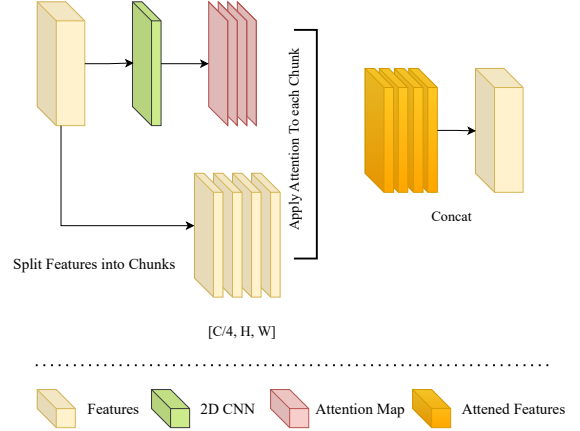


Figure 3. Illustration of the spatial attention mechanism in the proposed MSAGSM module. Feature maps from the 2D CNN are divided into multiple channel-wise chunks (e.g., $C/4$ per group). Each chunk is processed independently through a spatial attention module to highlight relevant regions (e.g., players, ball) while suppressing background noise. The attended features are then concatenated and forwarded to the temporal modeling block.

ing it to focus on different regions as needed, and offering greater flexibility and expressiveness across diverse sporting contexts.

For each head, a 2D convolutional layer generates a spatial attention map based on the original features. These maps are applied independently to their corresponding feature chunks, allowing each head to specialize in distinct spatial regions in a data-driven manner. Finally, the attended feature chunks are concatenated to reconstruct a unified, refined feature representation.

3.3. MultiScale GSM

We adopt the GSM as a reference architecture, as it has been proven effective in the PES domain [11, 29, 35]. GSM performs a gating-based temporal shifting mechanism inspired by TSM [15] and GST [19]. However, a key limitation of GSM is that it only performs shifts across adjacent frames, restricting its ability to capture longer-range temporal dependencies directly, which is often important in sports videos to classify events and discriminate similar frames.

We propose the MSAGSM, which extends GSM by replacing fixed, adjacent-frame shifting with a learnable, spatially-aware gating mechanism that enables direct access to longer temporal ranges. The architectural design of MSAGSM is illustrated in Figure 4.

Given a sequence of feature maps $X \in \mathbb{R}^{C \times T \times H \times W}$, where C is the number of channels, and T , H , W denote the temporal length, height, and width, respectively. For each temporal dilation scale, MSGSM first applies a

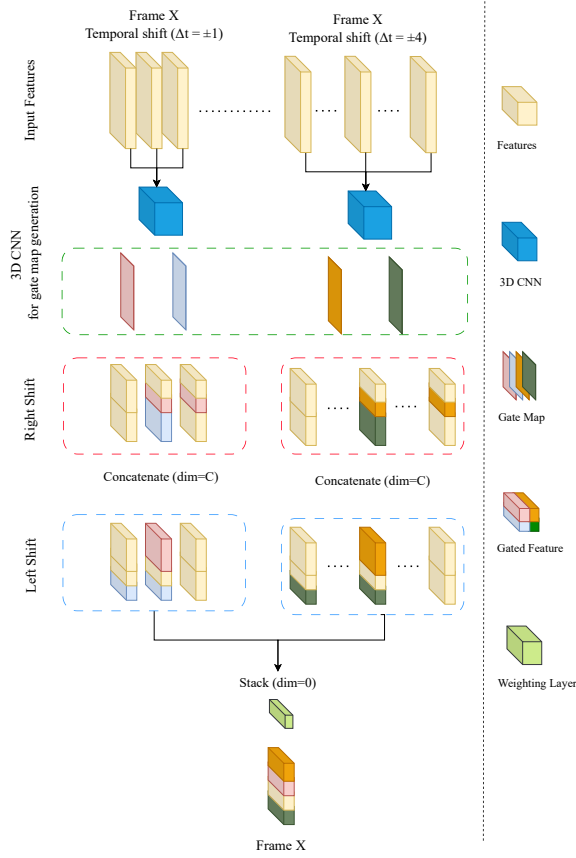


Figure 4. Structure of the proposed Multi-Scale Gate Shift Module (MSGSM). Given input features, a 3D CNN generates gate maps corresponding to different temporal shift ranges (e.g., $\Delta t = \pm 1, \pm 2$). Features are shifted left and right across multiple scales, gated accordingly, and combined through concatenation and stacking. This design enables the model to adaptively capture short- and long-term temporal dependencies in a data-driven manner.

gating layer implemented as a 3D CNN. This gating layer receives a temporal window of three feature maps sampled across time (with dilation) centered around the current timestamp. Two gating maps are then generated for each feature map—corresponding to left and right shifts. These gates are activated using the \tanh function to constrain their values between $(-1, +1)$, ensuring stable modulation. ($G_{\text{left}}, G_{\text{right}} = \tanh(\text{Conv3D}(X))$).

The feature map is split into two groups $X = [X_{\text{left}}, X_{\text{right}}]$, each modulated by one of the gates and then temporally shifted left or right via a rolling operation

$$\hat{X}_{\text{left}} = \text{Roll}(X_{\text{left}} \odot G_{\text{left}}, -\delta) \quad (1)$$

$$\hat{X}_{\text{right}} = \text{Roll}(X_{\text{right}} \odot G_{\text{right}}, +\delta) \quad (2)$$

Padding is applied to maintain shape integrity and pre-

vent feature loss at the sequence boundaries. To preserve important information, the shifted features are added back to the original input via a residual connection. The gated, shifted features are then concatenated along the channel dimension to restore the original shape. $\hat{X} = [\hat{X}_{\text{left}}, \hat{X}_{\text{right}}] + X$

Finally, the outputs from different dilation levels are stacked along a new dimension and passed through a learnable weighting mechanism. This layer adaptively determines the importance of each temporal scale, enabling the model to incorporate information across varying temporal distances. Formally, let $\{\hat{X}^{(i)}\}_{i=1}^N$ denote the outputs from N different shift ranges. The final output is computed as:

$$\hat{X}_{\text{final}} = \sum_{i=1}^N w_i \cdot \hat{X}^{(i)}, \quad \text{where } \sum_{i=1}^N w_i = 1, w_i \geq 0 \quad (3)$$

Here, w_i are learnable scalar weights normalized via a softmax function. This design allows the model to emphasize the most relevant temporal scales while introducing only minimal computational overhead compared to the original GSM.

4. Empirical Study

Examples of TTA Dataset

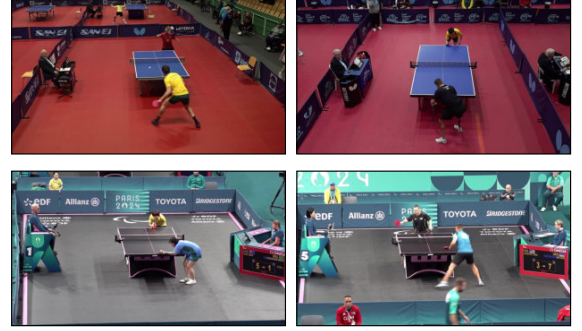


Figure 5. Example frames from the proposed TTA dataset. The top row shows samples from World Para Table Tennis (WPF) matches, while the bottom row displays clips from the 2024 Paris Paralympic Games. The dataset captures diverse viewing angles, frequent occlusions, and high event density representative of real-world elite-level table tennis.

In this section, we first review all the datasets used to evaluate the proposed MSAGSM, with a detailed description of the newly introduced TTA dataset. We then outline the implementation details of our method, conduct an ablation study to analyze the contribution of each module component, and finally present a comparative evaluation against prior methods and current state-of-the-art approaches.

4.1. Datasets

We evaluate our method on four fine-grained sports video datasets with frame-level annotations: Tennis [40], Figure Skating [10], FineDiving [38], and our proposed Table Tennis Australia (TTA) dataset.

The Tennis dataset consists of 3,345 video clips from 28 matches, with frame rates of 25 or 30 FPS. It contains 33,791 frame-accurate annotations spanning six event classes. The Figure Skating dataset includes 11 broadcast videos (all 25 FPS), covering 371 short program performances from major international competitions between 2010 and 2019. It includes 3,674 annotated events across four classes. Following previous work [10, 29, 35], we adopt two evaluation splits: a competition split (FS-Comp) and a performance split (FS-Perf). The FineDiving dataset contains 3,000 diving clips with temporal segment annotations. These have been converted into frame-level event labels across four classes using the annotation protocol from [11].

We also introduce the Table Tennis Australia (TTA) dataset, the first precise event spotting benchmark for table tennis. It consists of 39 full-game videos recorded at 30 FPS, totaling 4,878 annotated events across 8 classes: serve, bounce, forehand, and backhand, each labeled separately for near and far sides of the table. Examples of the TTA dataset are presented in Figure 5. Events are annotated following labeling protocols from Table Tennis Australia. For example, a frame is labeled as an event when the ball contacts the paddle or undergoes significant motion immediately after. In cases of occlusion (e.g., when a player blocks the ball near the camera), temporal context from preceding and following frames is used to estimate the most accurate event frame. For more details, please refer to the supplementary materials.

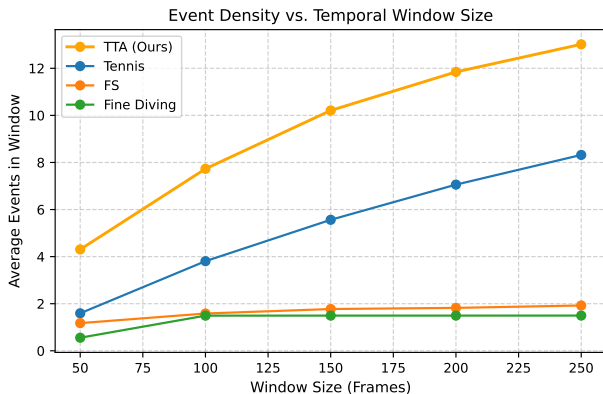


Figure 6. Comparison of event density (average number of events) across varying temporal window sizes. TTA shows the highest event density across all ranges, reflecting its fine-grained and fast-paced nature.

Unlike existing datasets, TTA videos are collected using handheld cameras by professional analysts from Paralympics Australia. The dataset includes elite-level competitions such as the Paralympics and WPF. This real-world, single-camera setting introduces challenges such as frequent occlusions, motion blur, and dynamic angles—conditions closer to practical applications—unlike the broadcast-quality videos used in most prior work. As shown in Figure 6, TTA exhibits the highest event density among all datasets, averaging 7.73 events per 100-frame window, compared to 3.81 in Tennis and significantly fewer in others. This emphasizes the need for models that can capture fine-grained temporal structure and distinguish between visually similar frames within narrow time intervals.

4.2. Evaluation

Since our proposed module, MSAGSM, is designed to be a lightweight and drop-in replacement for GSM, we follow the same training procedure as the E2E-Spot baseline [11], replacing GSM with MSAGSM in the backbone. The model performance is evaluated using the mean Average Precision (mAP), computed by averaging the Average Precision (AP) across all event classes. Following prior work, we report results under two temporal tolerance settings: $\delta = 1$ and $\delta = 2$, representing correct prediction within 1 frame distance and 2 frame distances.

4.3. Implementation Details

We follow the training protocol established in E2E-Spot. All models are trained using input clips of length $L = 100$ frames and a batch size of 8. Each epoch comprises 5,000 clips randomly sampled from the training set. Training is conducted for 50 epochs using the AdamW optimizer [18] with a base learning rate of 1×10^{-3} . We apply 3 warm-up epochs followed by a cosine decay schedule. To address class imbalance, positive classes in the cross-entropy loss are weighted by a factor of $w = 5$. We evaluate our MSAGSM module using two backbone architectures—RegNetY-200 [21] and ResNet-18 [9]—both adopted from the original E2E framework. All experiments are conducted on a single NVIDIA A100 GPU.

4.4. Comparison with State-of-the-Art

To assess the effectiveness and generalizability of MSAGSM, we compare it with three representative models in the PES literature: **E2E-Spot**, **T-DEED**, and **UGLF**. All three models follow a common architectural structure: a 2D backbone for feature extraction, followed by a temporal modeling module, and a decoder for frame-level prediction. E2E-Spot serves as a strong baseline due to its simplicity and broad adoption in the field, while T-DEED and UGLF build upon E2E by introducing additional modules or input features to model long-range dependencies or en-

Table 1. Performance comparison (mAP %) under different temporal tolerances ($\delta = 1$ and $\delta = 2$). Results are reported on five fine-grained sports video datasets. The best result for each column is **bolded**, and our proposed method is *italicized*. \star indicates the best result within each model-backbone group. All models are evaluated using a fixed clip length of 100 frames.

Model	Backbone	Temp Module	TTA		Tennis		FS.Comp		FS.Perf		FineDiving		Parameters
			$\delta=1$	$\delta=2$	$\delta=1$	$\delta=2$	$\delta=1$	$\delta=2$	$\delta=1$	$\delta=2$	$\delta=1$	$\delta=2$	
E2E-Spot	RegNetY-200	GSM	66.42	76.90	90.03	96.48	75.39	89.33	81.27	94.14	67.89	86.97	4.45M
E2E-Spot	RegNetY-200	GSF	63.70	72.19	89.01	96.55 \star	75.49	89.32	81.55	94.02	67.57	86.22	4.45M
<i>E2E-Spot</i>	<i>RegNetY-200</i>	<i>Ours</i>	<i>69.50\star</i>	<i>78.12\star</i>	<i>91.34\star</i>	<i>96.51</i>	<i>77.72\star</i>	<i>90.04\star</i>	<i>84.12\star</i>	<i>96.90\star</i>	<i>71.03\star</i>	<i>87.26\star</i>	<i>4.50M</i>
T-DEED	RegNetY-200	GSM	60.69	69.30	89.21	97.15 \star	71.69	90.02	66.18	84.02	66.18	84.02	16.42M
T-DEED	RegNetY-200	GSF	54.04	64.51	89.58	97.06	75.52	92.15\star	79.82	94.79\star	67.04\star	83.24	16.42M
<i>T-DEED</i>	<i>RegNetY-200</i>	<i>Ours</i>	<i>63.52\star</i>	<i>71.16\star</i>	<i>90.68\star</i>	<i>96.67</i>	<i>75.55\star</i>	<i>87.61</i>	<i>82.41\star</i>	<i>94.12</i>	<i>66.70</i>	<i>84.60\star</i>	<i>16.48M</i>
UGLF	RegNetY-200	GSM	63.52	71.16	89.73	97.16\star	77.25	90.44	79.24	93.08	66.88	84.94	4.45M
UGLF	RegNetY-200	GSF	63.70	72.19	89.39	97.06	72.61	86.90	82.06	94.38	66.65	84.27	4.45M
<i>UGLF</i>	<i>RegNetY-200</i>	<i>Ours</i>	<i>64.82\star</i>	<i>74.84\star</i>	<i>90.98\star</i>	<i>97.10</i>	<i>78.86\star</i>	<i>91.13\star</i>	<i>82.64\star</i>	<i>96.12\star</i>	<i>67.21\star</i>	<i>85.34\star</i>	<i>4.50M</i>

hance feature discrimination (e.g., via SGP, GLIP). Each method adopts a different temporal modeling choice—E2E and UGLF both report GSM as their best-performing module, while T-DEED employs GSF. Additionally, all three models use **RegNetY-200** as their 2D backbone of choice, based on reported performance in their original implementations. To ensure fairness, we reused the officially released codebases and trained each model on our hardware under consistent settings. For each, we report the best performance across multiple runs.

Main Results. Table 1 presents results on five fine-grained sports video datasets under two temporal tolerance thresholds ($\delta = 1$ and $\delta = 2$). Across the board, our proposed MSAGSM module consistently outperforms existing temporal modeling approaches. For example, within the E2E architecture using RegNetY-200, MSAGSM improves upon GSM by **+3.08** mAP on TTA at $\delta = 1$, and by **+1.15** on FineDiving at $\delta = 1$. Similar performance gains are observed when MSAGSM replaces the original temporal module in more complex models such as T-DEED and UGLF.

Out of 30 possible comparisons across model-backbone configurations, MSAGSM achieves the best result in **24** cases when compared directly against other temporal modules. Furthermore, it ranks first in **8 out of 10** columns when considering overall best scores, setting new state-of-the-art performance simply by replacing the temporal component.

Backbone and Module Versatility. To evaluate the generality of our approach, we further experiment with alternative backbones—specifically ResNet-18—in E2E, T-DEED, and UGLF architectures. For simplicity, the main table includes RegNetY-200 results only, while additional results for E2E, T-DEED and UGLF with ResNet-18 are provided in the supplementary materials. We also evaluate alternative temporal modules not originally reported in the respective papers: GSF in E2E and UGLF, and GSM in T-DEED. Across all these configurations, MSAGSM consistently delivers strong performance without increasing

model complexity, demonstrating its robustness and adaptability. For both E2E-Spot and UGLF, which are relatively simpler models, our MSAGSM module demonstrates strong improvements over their original temporal module designs. Specifically, E2E-Spot with MSAGSM outperforms all other temporal modules across all five datasets, while UGLF with MSAGSM achieves the best performance in 9 out of 10 groups. We observe that the improvement is less pronounced in the T-DEED model, which is reasonable given that T-DEED already incorporates a more complex temporal modeling design. In such cases, introducing MSAGSM may add redundant or conflicting temporal information, which could complicate effective feature retrieval.

Efficiency. MSAGSM maintains a lightweight footprint, using only **4.5M** parameters in its default configuration. This matches or only slightly exceeds the size of existing temporal modules, while consistently delivering superior accuracy. Its compact design makes MSAGSM a practical drop-in replacement for both lightweight and large-scale models that rely on 2D pretrained CNN backbones.

Summary. These results demonstrate the effectiveness of MSAGSM as a robust and efficient temporal modeling module. Its consistent improvements across diverse models and baseline temporal modules, particularly on our proposed **TTA** benchmark (see Figure 6), underscore its suitability for capturing the high-frequency, fine-grained temporal dynamics inherent in sports video understanding.

4.5. Ablation Study

We conduct ablation studies on the **TTA** and **FineDiving** datasets, which represent two contrasting types of sports—one with high event density and the other with sparse events. These experiments evaluate two key components of our proposed MSAGSM: the number of attention heads and the temporal window size (i.e., dilation range).

Number of Attention Heads. We fix the dilation setting to $[1, 2, 3]$ and vary the number of attention heads. As

Table 2. Ablation study on attention head count and dilation range using the MSAGSM module on the TTA and FineDiving datasets. All results are reported in mAP (%).

Setting	Value	TTA		FineDiving		Params
		mAP@1	mAP@2	mAP@1	mAP@2	
Varying Number of Attention Heads (Dilations = [1,2,3])						
Heads	1	60.99	75.38	66.36	83.47	4.50M
Heads	2	69.50 (+8.51)	78.12 (+2.74)	71.03 (+4.67)	87.26 (+3.79)	4.51M
Heads	3	65.87 (+4.88)	75.87 (+0.49)	67.93 (+1.57)	85.11 (+1.64)	4.51M
Heads	4	61.01 (+0.02)	72.98 (−2.40)	68.72 (+2.36)	85.16 (+1.69)	4.52M
Heads	8	64.19 (+3.20)	72.94 (−2.44)	70.06 (+3.70)	85.91 (+2.44)	4.55M
Varying Temporal Window Size (Heads = 2)						
Distance	[1,2]	60.78	71.10	68.56	85.49	4.48M
Distance	[1,2,3]	69.50 (+8.72)	78.12 (+7.02)	71.03 (+2.47)	87.26 (+1.77)	4.51M
Distance	[1,...,4]	64.18 (+3.40)	71.59 (+0.49)	69.02 (+0.46)	85.17 (-0.32)	4.53M
Distance	[1,...,5]	67.54 (+6.76)	67.41 (-3.69)	69.26 (+0.70)	85.26 (-0.23)	4.55M
Distance	[1,...,6]	64.03 (+3.25)	75.38 (+4.28)	69.84 (+1.28)	85.34 (-0.15)	4.57M

shown in Table 6, using two heads achieves the best trade-off across both datasets. On TTA, increasing from one to two heads substantially improves mAP by +8.51 and +2.74 at $\delta = 1$ and $\delta = 2$, respectively. However, increasing the number of heads beyond two leads to inconsistent or diminished performance, likely due to over-fragmentation of attention across feature subspaces. On FineDiving, which contains smoother and more globally distributed motion, two heads also yield the best result (71.03 mAP@1), with additional heads offering minimal or no further gains.

Temporal Window Size. We fix the number of heads at two and vary the dilation configurations to control the size of the temporal receptive field. The default setting [1, 2, 3] performs best overall. Slight improvements are observed on TTA with longer ranges (e.g., [1, 2, 3, 4], +3.40 mAP@1), but extremely long windows such as [1, ..., 6] result in diminishing or inconsistent gains. This suggests that overly large temporal windows may dilute fine-grained event cues. These findings highlight the importance of balancing broad context modeling with temporal precision.

In summary, MSAGSM achieves strong and stable performance with two attention heads and a temporal window of [1, 2, 3], demonstrating its robustness across datasets with diverse temporal dynamics. Additional ablation results, including further window configurations, are provided in the supplementary materials.

5. Discussion

In this paper, we presented MSAGSM, a plug-and-play temporal module designed for integration with 2D backbone feature extractors in temporally stringent event spotting tasks. MSAGSM is a simple yet effective component

that enhances models following the E2E-Spot framework [11], enabling improved performance—particularly on temporally precise spotting tasks in fine-grained sports videos. Our method consistently outperforms existing temporal modules such as GSM and GSF across various settings, including different backbones (e.g., RegNetY-200, ResNet-18) and model architectures (e.g., T-DEED, UGLF). Details and additional experiments, including results on ResNet-18 backbones, are provided in the supplementary materials.

The design of MSAGSM enables rich temporal modeling with minimal additional computational overhead, making it a practical choice for real-world applications. We observe that MSAGSM performs particularly well when paired with both stronger backbone architectures and simpler models, suggesting that stronger feature representations further amplify the module’s ability to capture temporal dynamics.

In addition, we introduce the **TTA** dataset—the first table tennis dataset for PES—which brings unique challenges due to its high event density and rapid scene changes. We hope this dataset will serve as a new benchmark to advance research in this domain.

While our work focuses on PES, MSAGSM has potential for broader video understanding tasks, such as video action recognition (VAR). Unlike PES, VAR typically uses sparse frame sampling, which may limit its temporal precision. Future work will explore how fine-grained modules like MSAGSM can bridge this gap and enhance VAR performance.

Overall, we envision MSAGSM as a lightweight, general-purpose temporal module that can be easily integrated into existing pipelines to improve fine-grained temporal reasoning in video understanding.

6. Conclusion

We introduce a simple yet effective temporal module, the MSAGSM, which can be seamlessly integrated into any existing 2D backbone feature extractor to enable multi-scale temporal modeling. MSAGSM leverages both multi-scale temporal shifts and an attention mechanism to selectively aggregate information across frames at varying temporal distances. We conduct extensive evaluations across five fine-grained sports video datasets for PES, demonstrating that MSAGSM consistently enhances model performance and achieves state-of-the-art results. For instance, when integrated into E2E-Spot, MSAGSM yields an absolute improvement of **+3.08%** mAP@1 on the TTA dataset, while introducing only **0.01M** additional parameters. Furthermore, we propose **TTA**, a new PES benchmark dataset in the domain of table tennis, designed to encourage future research on fine-grained and high-frequency sports video understanding.

References

- [1] Mengqi Cao, Min Yang, Guozhen Zhang, Xiaotian Li, Yilu Wu, Gangshan Wu, and Limin Wang. Spotformer: A transformer-based framework for precise soccer action spotting. In *2022 IEEE 24th International Workshop on Multimedia Signal Processing (MMSP)*, pages 1–6. IEEE, 2022. 1
- [2] Bo Chen, Fangzhou Meng, Hongying Tang, and Guanjun Tong. Two-level attention module based on spurious-3d residual networks for human action recognition. *Sensors*, 23(3):1707, 2023. 2
- [3] Long Chen, Hanwang Zhang, Jun Xiao, Liqiang Nie, Jian Shao, Wei Liu, and Tat-Seng Chua. Sca-cnn: Spatial and channel-wise attention in convolutional networks for image captioning. In *Proceedings of the IEEE conference on computer vision and pattern recognition*, pages 5659–5667, 2017. 4
- [4] Julien Denize, Mykola Liashuha, Jaonary Rabarisoa, Astrid Orcesi, and Romain Hérault. Comedian: Self-supervised learning and knowledge distillation for action spotting using transformers. In *Proceedings of the IEEE/CVF Winter Conference on Applications of Computer Vision*, pages 530–540, 2024. 1
- [5] Alexey Dosovitskiy, Lucas Beyer, Alexander Kolesnikov, Dirk Weissenborn, Xiaohua Zhai, Thomas Unterthiner, Mostafa Dehghani, Matthias Minderer, Georg Heigold, Sylvain Gelly, et al. An image is worth 16x16 words: Transformers for image recognition at scale. *arXiv preprint arXiv:2010.11929*, 2020. 2, 4
- [6] Haoqi Fan, Bo Xiong, Karttikeya Mangalam, Yanghao Li, Zhicheng Yan, Jitendra Malik, and Christoph Feichtenhofer. Multiscale vision transformers. In *Proceedings of the IEEE/CVF international conference on computer vision*, pages 6824–6835, 2021. 2
- [7] Christoph Feichtenhofer, Haoqi Fan, Jitendra Malik, and Kaiming He. Slowfast networks for video recognition. In *Proceedings of the IEEE/CVF international conference on computer vision*, pages 6202–6211, 2019. 3
- [8] Silvio Giancola, Mohieddine Amine, Tarek Dghaily, and Bernard Ghanem. Soccernet: A scalable dataset for action spotting in soccer videos. In *Proceedings of the IEEE conference on computer vision and pattern recognition workshops*, pages 1711–1721, 2018. 2, 3
- [9] Kaiming He, Xiangyu Zhang, Shaoqing Ren, and Jian Sun. Deep residual learning for image recognition. In *Proceedings of the IEEE conference on computer vision and pattern recognition*, pages 770–778, 2016. 6, 11
- [10] James Hong, Matthew Fisher, Michaël Gharbi, and Kayvon Fatahalian. Video pose distillation for few-shot, fine-grained sports action recognition. In *Proceedings of the IEEE/CVF International Conference on Computer Vision*, pages 9254–9263, 2021. 2, 3, 6
- [11] James Hong, Haotian Zhang, Michaël Gharbi, Matthew Fisher, and Kayvon Fatahalian. Spotting temporally precise, fine-grained events in video. In *European Conference on Computer Vision*, pages 33–51. Springer, 2022. 1, 2, 3, 4, 6, 8, 11
- [12] Boyuan Jiang, MengMeng Wang, Weihao Gan, Wei Wu, and Junjie Yan. Sstm: Spatiotemporal and motion encoding for action recognition. In *Proceedings of the IEEE/CVF international conference on computer vision*, pages 2000–2009, 2019. 2
- [13] Dan Kondratyuk, Liangzhe Yuan, Yandong Li, Li Zhang, Mingxing Tan, Matthew Brown, and Boqing Gong. Movinets: Mobile video networks for efficient video recognition. In *Proceedings of the IEEE/CVF conference on computer vision and pattern recognition*, pages 16020–16030, 2021. 3
- [14] Liunian Harold Li, Pengchuan Zhang, Haotian Zhang, Jianwei Yang, Chunyuan Li, Yiwu Zhong, Lijuan Wang, Lu Yuan, Lei Zhang, Jenq-Neng Hwang, et al. Grounded language-image pre-training. In *Proceedings of the IEEE/CVF conference on computer vision and pattern recognition*, pages 10965–10975, 2022. 3
- [15] Ji Lin, Chuang Gan, and Song Han. Tsm: Temporal shift module for efficient video understanding. In *Proceedings of the IEEE/CVF international conference on computer vision*, pages 7083–7093, 2019. 3, 4
- [16] Tianwei Lin, Xu Zhao, Haisheng Su, Chongjing Wang, and Ming Yang. Bsn: Boundary sensitive network for temporal action proposal generation. In *Proceedings of the European conference on computer vision (ECCV)*, pages 3–19, 2018. 3
- [17] Ze Liu, Jia Ning, Yue Cao, Yixuan Wei, Zheng Zhang, Stephen Lin, and Han Hu. Video swin transformer. In *Proceedings of the IEEE/CVF conference on computer vision and pattern recognition*, pages 3202–3211, 2022. 2
- [18] Ilya Loshchilov and Frank Hutter. Decoupled weight decay regularization. *arXiv preprint arXiv:1711.05101*, 2017. 6
- [19] Chenxu Luo and Alan L Yuille. Grouped spatial-temporal aggregation for efficient action recognition. In *Proceedings of the IEEE/CVF international conference on computer vision*, pages 5512–5521, 2019. 3, 4
- [20] Zhaofan Qiu, Ting Yao, and Tao Mei. Learning spatiotemporal representation with pseudo-3d residual networks.

- In *proceedings of the IEEE International Conference on Computer Vision*, pages 5533–5541, 2017. 2
- [21] Ilija Radosavovic, Raj Prateek Kosaraju, Ross Girshick, Kaiming He, and Piotr Dollár. Designing network design spaces. In *Proceedings of the IEEE/CVF conference on computer vision and pattern recognition*, pages 10428–10436, 2020. 6, 11
- [22] Dian Shao, Yue Zhao, Bo Dai, and Dahua Lin. Finegym: A hierarchical video dataset for fine-grained action understanding. In *Proceedings of the IEEE/CVF conference on computer vision and pattern recognition*, pages 2616–2625, 2020. 2, 3
- [23] Dingfeng Shi, Yujie Zhong, Qiong Cao, Lin Ma, Jia Li, and Dacheng Tao. Tridet: Temporal action detection with relative boundary modeling. In *Proceedings of the IEEE/CVF Conference on Computer Vision and Pattern Recognition*, pages 18857–18866, 2023. 3
- [24] Haisheng Su, Weihao Gan, Wei Wu, Yu Qiao, and Junjie Yan. Bsn++: Complementary boundary regressor with scale-balanced relation modeling for temporal action proposal generation. In *Proceedings of the AAAI conference on artificial intelligence*, pages 2602–2610, 2021. 3
- [25] Swathikiran Sudhakaran, Sergio Escalera, and Oswald Lanz. Gate-shift networks for video action recognition. In *Proceedings of the IEEE/CVF conference on computer vision and pattern recognition*, pages 1102–1111, 2020. 1, 3
- [26] Swathikiran Sudhakaran, Sergio Escalera, and Oswald Lanz. Gate-shift-fuse for video action recognition. *IEEE Transactions on Pattern Analysis and Machine Intelligence*, 45(9): 10913–10928, 2023. 3
- [27] Zhan Tong, Yibing Song, Jue Wang, and Limin Wang. Videomae: Masked autoencoders are data-efficient learners for self-supervised video pre-training. *Advances in neural information processing systems*, 35:10078–10093, 2022. 2
- [28] Du Tran, Heng Wang, Lorenzo Torresani, Jamie Ray, Yann LeCun, and Manohar Paluri. A closer look at spatiotemporal convolutions for action recognition. In *Proceedings of the IEEE conference on Computer Vision and Pattern Recognition*, pages 6450–6459, 2018. 2
- [29] Kim Hoang Tran, Phuc Vuong Do, Ngoc Quoc Ly, and Ngan Le. Unifying global and local scene entities modelling for precise action spotting. In *2024 International Joint Conference on Neural Networks (IJCNN)*, pages 1–8. IEEE, 2024. 1, 3, 4, 6, 11
- [30] Bastien Vanderplaetse and Stephane Dupont. Improved soccer action spotting using both audio and video streams. In *Proceedings of the IEEE/CVF Conference on Computer Vision and Pattern Recognition Workshops*, pages 896–897, 2020. 1
- [31] Limin Wang, Yuanjun Xiong, Zhe Wang, Yu Qiao, Dahua Lin, Xiaoou Tang, and Luc Van Gool. Temporal segment networks: Towards good practices for deep action recognition. In *European conference on computer vision*, pages 20–36. Springer, 2016. 3
- [32] Qilong Wang, Banggu Wu, Pengfei Zhu, Peihua Li, Wangmeng Zuo, and Qinghua Hu. Eca-net: Efficient channel attention for deep convolutional neural networks. In *Proceedings of the IEEE/CVF conference on computer vision and pattern recognition*, pages 11534–11542, 2020. 4
- [33] Sanghyun Woo, Jongchan Park, Joon-Young Lee, and In So Kweon. Cbam: Convolutional block attention module. In *Proceedings of the European conference on computer vision (ECCV)*, pages 3–19, 2018. 4
- [34] Artur Xarles, Sergio Escalera, Thomas B Moeslund, and Albert Clapés. Astra: An action spotting transformer for soccer videos. In *Proceedings of the 6th International Workshop on Multimedia Content Analysis in Sports*, pages 93–102, 2023. 1, 3
- [35] Artur Xarles, Sergio Escalera, Thomas B Moeslund, and Albert Clapés. T-deed: Temporal-discriminability enhancer encoder-decoder for precise event spotting in sports videos. In *Proceedings of the IEEE/CVF Conference on Computer Vision and Pattern Recognition*, pages 3410–3419, 2024. 1, 2, 3, 4, 6, 11
- [36] Saining Xie, Chen Sun, Jonathan Huang, Zhuowen Tu, and Kevin Murphy. Rethinking spatiotemporal feature learning: Speed-accuracy trade-offs in video classification. In *Proceedings of the European conference on computer vision (ECCV)*, pages 305–321, 2018. 2
- [37] Hao Xu, Arbind Agrahari Baniya, Sam Well, Mohamed Reda Bouadjene, Richard Dazeley, and Sunil Aryal. Action spotting and precise event detection in sports: Datasets, methods, and challenges. *arXiv preprint arXiv:2505.03991*, 2025. 3
- [38] Jinglin Xu, Yongming Rao, Xumin Yu, Guangyi Chen, Jie Zhou, and Jiwen Lu. Finediving: A fine-grained dataset for procedure-aware action quality assessment. In *Proceedings of the IEEE/CVF conference on computer vision and pattern recognition*, pages 2949–2958, 2022. 2, 3, 6
- [39] Hongyi Zhang, Moustapha Cisse, Yann N Dauphin, and David Lopez-Paz. mixup: Beyond empirical risk minimization. *arXiv preprint arXiv:1710.09412*, 2017. 11
- [40] Haotian Zhang, Cristobal Sciotto, Maneesh Agrawala, and Kayvon Fatahalian. Vid2player: Controllable video sprites that behave and appear like professional tennis players. *ACM Transactions on Graphics (TOG)*, 40(3):1–16, 2021. 6
- [41] He Zhu, Junwei Liang, Chengzhi Lin, Jun Zhang, and Jianming Hu. A transformer-based system for action spotting in soccer videos. In *Proceedings of the 5th international acm workshop on multimedia content analysis in sports*, pages 103–109, 2022. 1

A. Implementation Details

A.1. Backbone Model

In addition to the backbone model RegNetY-200 [21] used in all three original works—E2E-Spot [11], T-DEED [35], and UGLF [29]—we also experimented with ResNet-18 [9] as the backbone. MSAGSM is integrated into the backbone at each residual block.

A.2. Baselines

For all implementations, we adopted the publicly released code of each baseline whenever available and used the exact training configurations provided in their papers. We did observe minor performance drops compared to the results reported in the original papers, but these were marginal. Since our module is integrated directly into their official implementations without altering other components, we consider this a fair comparison.

Regarding UGLF [29], their paper utilizes additional GLIP-provided information, which is not publicly available. Therefore, we followed their released code without this input.

A.3. Training Configuration

All experiments were conducted on the same machine equipped with L40S GPUs to ensure consistency. The overall training configuration follows E2E-Spot: each epoch randomly samples 5,000 clips to reduce training time while maintaining good coverage of the dataset. To mitigate the imbalance between event and non-event frames, we applied a weight of $5\times$ to the event classes.

We trained for 50 epochs using AdamW with an initial learning rate of 1×10^{-3} , a batch size of 8, and 3 warm-up epochs. Cross-entropy loss was used, with input tensors shaped as $[B, T, C, H, W]$ (batch, time, channels, height, width) and output tensors as $[B, T, C]$, representing the frame-wise class probabilities after softmax.

A.4. Data Augmentations

During training, we randomly apply color jitter, Gaussian blur, and mixup [39]. On all datasets, frames of size 398×224 are randomly cropped to 224×224 pixels. The crop is applied only along the width dimension to preserve critical spatial information, as cropping the height could exclude important event regions. This also improves processing speed, since both the tennis court and table tennis table occupy the central region of the frame.

B. TTA Dataset

We introduce the Table Tennis Australia (TTA) dataset, the first benchmark dataset for table tennis in the PES task.

All videos in the TTA dataset were recorded and provided by the Paralympics Table Tennis Australia team. The

Occluded Event Examples



Figure 7. Examples of occluded events, when events happened during occlusion.

dataset is intended strictly for research purposes and will be made publicly available upon request and approval.

It consists of 39 games, where each game is an 11-point set and each match is played as best-of-five games. We ensured diversity by including videos captured from different camera angles, with varying table and stadium colors, and across different competition levels—from elite Paralympics events to slightly lower-level WPF tournaments, which reflect broader public scenarios.

The dataset contains annotations for 8 action classes: *serve*, *forehand*, *backhand*, and *bounce*, each labeled separately for the *close table* and *far table*. Examples of each class are shown in Figure 8.

B.1. Dataset Annotation Details

Annotation was performed by three team members, with all annotations subsequently reviewed and verified by a professional sports analyst from Table Tennis Australia. For each event type, we annotated the exact frame corresponding to the critical action—for example, the frame when the ball contacts the bat for a serve, or when it lands on the table (accompanied by a sudden directional change) for a bounce.

We note that due to the frame rate of the videos, some critical moments might not be captured precisely as shown in Figure 7; in such cases, the closest possible frame was annotated. Another challenge arose from the consistent back-facing camera angle: certain events were occasionally blocked or occluded by players—such as close-table bounces or backhands. In these cases, following the procedure used by professional sports analysts, we inferred the event frame based on the surrounding context in adjacent frames.

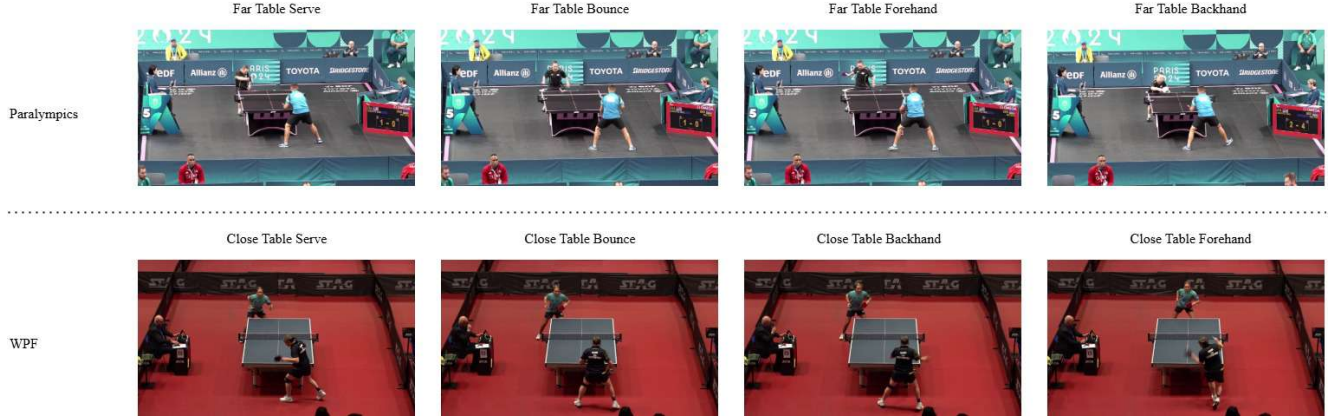


Figure 8. Examples from the TTA dataset. Each class is illustrated, with the top row showing examples from Paralympics matches and the bottom row from WPF tournaments.

Table 3. Performance comparison (mAP %) under different temporal tolerances ($\delta = 1$ and $\delta = 2$) for T-DEED and UGLF under ResNet-18 backbone. Results are reported on five fine-grained sports video datasets. The best result for each column is **bolded**, and our proposed method is *italicized*. \star indicates the best result within each model-backbone group. All models are evaluated using a fixed clip length of 100 frames.

Model	Backbone	Temp Module	TTA		Tennis		FS.Comp		FS.Perf		FineDiving		Parameters
			$\delta=1$	$\delta=2$	$\delta=1$	$\delta=2$	$\delta=1$	$\delta=2$	$\delta=1$	$\delta=2$	$\delta=1$	$\delta=2$	
E2E-Spot	ResNet-18	GSM	69.13	78.37	90.43	96.72	77.31	87.52	82.75	94.56	64.63	84.79	14.35M
E2E-Spot	ResNet-18	GSF	66.42	80.75*	90.48	97.01	73.21	87.37	78.50	90.58	64.25	84.01	14.35M
<i>E2E-Spot</i>	<i>ResNet-18</i>	<i>Ours</i>	70.49*	79.38	<i>90.81*</i>	<i>97.52*</i>	78.29*	90.93*	85.23*	96.62*	<i>67.17*</i>	<i>84.95*</i>	<i>14.37M</i>
T-DEED	ResNet-18	GSM	66.78	76.13	89.46*	97.19	76.65*	87.02	83.67*	95.35	63.11	83.34	37.34M
T-DEED	ResNet-18	GSF	68.84	75.59	88.48	97.22	75.58	88.87*	83.09	96.22	68.68*	85.21*	37.34M
<i>T-DEED</i>	<i>ResNet-18</i>	<i>Ours</i>	<i>69.92*</i>	<i>77.33*</i>	87.18	95.85*	76.17	88.57	82.58	96.35*	66.78	84.88	<i>37.37M</i>
UGLF	ResNet-18	GSM	60.05	69.50	89.38	97.14	75.93	90.16	81.28	92.60	65.88	84.92	14.35M
UGLF	ResNet-18	GSF	62.58*	68.57	89.11	97.31*	74.88	88.49	82.34*	94.27	65.56	84.56	14.35M
<i>UGLF</i>	<i>ResNet-18</i>	<i>Ours</i>	<i>62.30</i>	<i>72.14*</i>	91.06*	97.28	<i>77.21*</i>	<i>90.25*</i>	81.46	94.84*	68.98*	87.60*	<i>14.37M</i>

C. Additional Experiments

In this section, we provide additional experiments using ResNet-18 as the backbone within the E2E, T-DEED, and UGLF frameworks. We also report mAP@0 results across different temporal modules and datasets. Finally, we include results for alternative dilation configurations that were not shown in the main paper.

C.1. Different Backbone

We evaluate MSAGSM with ResNet-18 as the backbone to test its effectiveness with a different feature extractor. Results in Table 3 show that MSAGSM consistently improves performance across all models, confirming its robustness to backbone choice. Out of 10 results, MSAGSM achieves 8 best scores, and across 30 groups, it achieves 20 best results—particularly excelling in the simpler E2E and UGLF models. As observed in the main results, the additional temporal information from MSAGSM may conflict with the

more complex design of T-DEED, leading to less optimal gains in that setting. This suggests that T-DEED’s existing fine-grained temporal modules already capture much of the relevant temporal context, leaving little room for MSAGSM to contribute further. In some cases, the overlapping temporal mechanisms may introduce redundancy or even conflicting signals, which could hinder effective feature learning.

C.2. Exact Frame Prediction

In PES settings, mAP@0 measures whether the prediction lands exactly on the ground-truth frame. However, this is often ambiguous even for human annotators, so mAP@0 is considered a supplementary result. These results are presented in Table 4 for RegNetY-200 and Table 5 for ResNet-18.

We observe that even under the strict mAP@0 setting, MSAGSM achieves strong results: on RegNetY-200, it achieves the best result in 12 out of 15 cases, and on ResNet-18, in 10 out of 15 cases. This suggests that the

Table 4. Performance comparison (mAP %) under strict temporal tolerance ($\delta = 0$) for T-DEED and UGLF under RegNetY-200 backbone. Results are reported on five fine-grained sports video datasets. The best result for each column is **bolded**, and our proposed method is *italicized*. \star indicates the best result within each model-backbone group. All models are evaluated using a fixed clip length of 100 frames.

Model	Backbone	Temp Module	TTA	Tennis	FS_Comp	FS_Perf	FineDiving	Parameters
E2E-Spot	RegNetY-200	GSM	34.36	51.42	36.44	39.32	27.31	4.45M
E2E-Spot	RegNetY-200	GSF	36.17	49.68	36.25	40.07	29.41	4.45M
<i>E2E-Spot</i>	<i>RegNetY-200</i>	<i>Ours</i>	36.43\star	55.51\star	38.34\star	46.54\star	29.83\star	<i>4.50M</i>
T-DEED	RegNetY-200	GSM	33.32 \star	48.82	38.61	26.86	26.86	16.42M
T-DEED	RegNetY-200	GSF	26.27	50.08	38.83	38.89	28.50 \star	16.42M
<i>T-DEED</i>	<i>RegNetY-200</i>	<i>Ours</i>	<i>28.06</i>	<i>52.76\star</i>	<i>39.06\star</i>	<i>44.66\star</i>	<i>26.88</i>	<i>16.48M</i>
UGLF	RegNetY-200	GSM	34.36	50.31	36.99	38.29	27.11	4.45M
UGLF	RegNetY-200	GSF	36.17 \star	50.94	34.84	37.41	29.81	4.45M
<i>UGLF</i>	<i>RegNetY-200</i>	<i>Ours</i>	<i>33.93</i>	<i>53.10\star</i>	39.66\star	46.59\star	29.59\star	<i>4.50M</i>

Table 5. Performance comparison (mAP %) under strict temporal tolerance ($\delta = 0$) for T-DEED and UGLF under ResNet-18 backbone. Results are reported on five fine-grained sports video datasets. The best result for each column is **bolded**, and our proposed method is *italicized*. \star indicates the best result within each model-backbone group. All models are evaluated using a fixed clip length of 100 frames.

Model	Backbone	Temp Module	TTA	Tennis	FS_Comp	FS_Perf	FineDiving	Parameters
E2E-Spot	ResNet-18	GSM	40.30	49.74	37.80	43.73	26.53	14.35M
E2E-Spot	ResNet-18	GSF	39.11	49.32	35.50	39.04	24.31	14.35M
<i>E2E-Spot</i>	<i>ResNet-18</i>	<i>Ours</i>	43.81\star	52.82\star	40.49\star	45.75\star	30.43\star	<i>14.37M</i>
T-DEED	ResNet-18	GSM	39.81 \star	48.09	38.64 \star	42.82 \star	25.86 \star	37.34M
T-DEED	ResNet-18	GSF	38.26	45.57	35.54	42.03	28.81	37.34M
<i>T-DEED</i>	<i>ResNet-18</i>	<i>Ours</i>	<i>39.51</i>	<i>51.56\star</i>	<i>36.89</i>	<i>40.90</i>	<i>23.68</i>	<i>37.37M</i>
UGLF	ResNet-18	GSM	32.89	49.05	36.57	42.30 \star	24.53	14.35M
UGLF	ResNet-18	GSF	36.98	47.59	34.22	41.73	22.42	14.35M
<i>UGLF</i>	<i>ResNet-18</i>	<i>Ours</i>	<i>37.14\star</i>	<i>52.14\star</i>	40.69\star	<i>40.55</i>	<i>29.56\star</i>	<i>14.37M</i>

module is particularly effective at pinpointing exact event moments when integrated into simpler architectures such as E2E-Spot, as it can fully leverage its multi-scale shifts and spatial attention. In contrast, in more complex models like T-DEED—which already incorporate advanced temporal mechanisms—MSAGSM may partially overlap or conflict with existing components, slightly reducing its relative effectiveness.

C.3. Different Temporal Window Setting

Here, we present a more detailed evaluation of temporal window settings for MSAGSM, including wider ranges such as $[1, \dots, 9]$ and skipped patterns like $[1, 2, 4, 6]$. As longer temporal distances are incorporated, the improvements become unstable and often diminish, suggesting that

shifting information from nearby frames is sufficient in most cases. Notably, the configuration $[1, 2, 3]$ consistently performs best, effectively balancing short-term and moderate long-term dependencies. Smaller windows (like $[1, 2]$) fail to capture enough context, while larger windows (like $[1, \dots, 9]$) include redundant or noisy temporal information, which can confuse the model and harm precision. Thus, moderate dilation allows the model to attend to meaningful temporal cues without overfitting to irrelevant frames.

C.4. Class-wise Spotting Performance

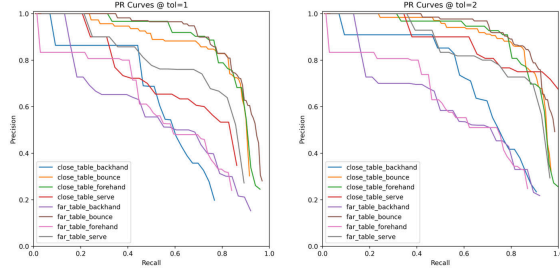
The difficulty of precisely spotting events varies across event classes. In Figure 9, we present the interpolated precision-recall curves for the different classes in the TTA,

Table 6. Ablation study on attention head count and dilation range using the MSAGSM module on the TTA and FineDiving datasets. All results are reported in mAP (%).

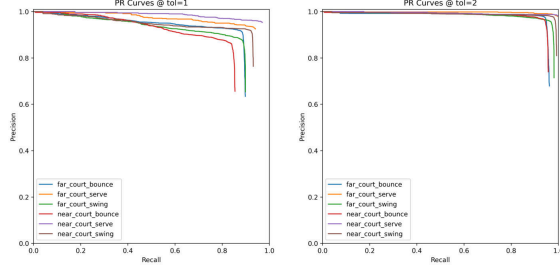
Setting	Value	TTA		FineDiving		Params
		mAP@1	mAP@2	mAP@1	mAP@2	
Varying Number of Attention Heads (Dilations = [1,2,3])						
Heads	1	60.99	75.38	66.36	83.47	4.50M
Heads	2	69.50 (+8.51)	78.12 (+2.74)	71.03 (+4.67)	87.26 (+3.79)	4.51M
Heads	3	65.87 (+4.88)	75.87 (+0.49)	67.93 (+1.57)	85.11 (+1.64)	4.51M
Heads	4	61.01 (+0.02)	72.98 (−2.40)	68.72 (+2.36)	85.16 (+1.69)	4.52M
Heads	8	64.19 (+3.20)	72.94 (−2.44)	70.06 (+3.70)	85.91 (+2.44)	4.55M
Varying Temporal Window Size (Heads = 2)						
Dilations	[1,2]	60.78	71.10	68.56	85.49	4.48M
Distance	[1,2,3]	69.50 (+8.72)	78.12 (+7.02)	71.03 (+2.47)	87.26 (+1.77)	4.51M
Dilations	[1,3,5]	68.14 (+7.36)	75.26 (+4.16)	68.18 (−0.34)	85.26 (−0.23)	4.51M
Distance	[1,...,4]	64.18 (+3.40)	71.59 (+0.49)	69.02 (+0.46)	85.17 (−0.32)	4.53M
Dilations	[1,2,4,6]	68.27 (+7.49)	75.07 (+3.97)	69.85 (+1.29)	87.02 (+1.53)	4.53M
Distance	[1,...,5]	67.54 (+6.76)	67.41 (−3.69)	69.26 (+0.70)	85.26 (−0.23)	4.55M
Distance	[1,...,6]	64.03 (+3.25)	75.38 (+4.28)	69.84 (+1.28)	85.34 (−0.15)	4.57M
Dilations	[1,...,9]	67.32 (+6.54)	76.44 (+5.34)	65.47 (−3.09)	82.80 (−3.97)	4.63M

Tennis, Figure Skating, and FineDiving datasets, as predicted by our default MSAGSM-E2E model.

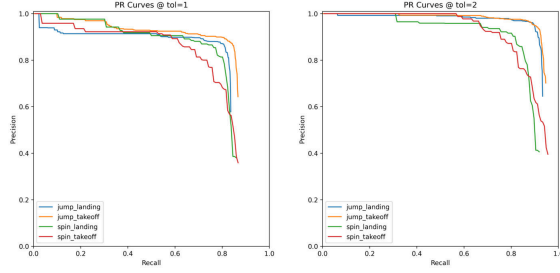
We show both curves at a tolerance of 1 and a tolerance of 2. In the TTA dataset, the model exhibits difficulties with both-sides backhand events, while performing particularly well on bounce events. A similar pattern is observed in the Tennis dataset. This is reasonable, as bounce frames typically exhibit a distinct characteristic of sudden motion change at the ball’s location, making them easier to detect. In contrast, distinguishing between forehand and backhand is often ambiguous because some players are left-handed and others are right-handed, making the visual cues less consistent for the model.



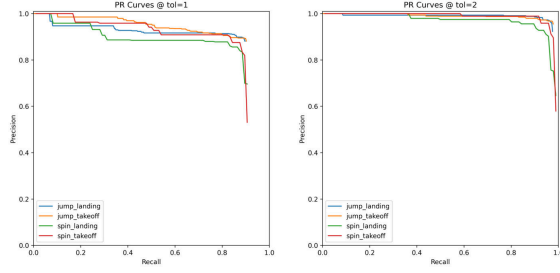
(a) TTA Curve



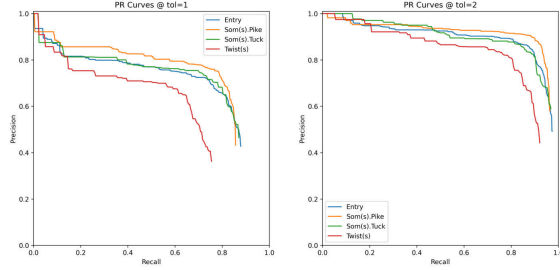
(b) Tennis Curve



(c) FS Comp Curve



(d) FS Perf Curve



(e) FineDiving Curve

Figure 9. Precision-Recall curves for different datasets. The left plot shows results at a tolerance of 1, and the right plot at a tolerance of 2.